IEEE Open Journal of
Antennas and Propagation

Received XX Month, 2023; revised XX Month, 2023; accepted XX Month, 2023; Date of publication XX Month, 2023; date of current version XX Month, 2023.

Digital Object Identifier 10.1109/OJAP.xxxx.xxxxxxx

Tuning-Range Extension Strategies for Varactor-Based Frequency-Reconfigurable Antennas

QUOC HUNG DANG[1], (Member, IEEE), NGHIA NGUYEN-TRONG[1], (Senior Member, IEEE), CHRISTOPHE FUMEAUX[3,1], (Fellow, IEEE), AND SHENGJIAN JAMMY CHEN[2,1], (Member, IEEE)

[1]School of Electrical & Mechanical Engineering, The University of Adelaide, Adelaide, 5005, SA, Australia
[2]The College of Science and Engineering, Flinders University, Tonsley, 5042, SA, Australia
[3]School of Electrical Engineering and Computer Science, The University of Queensland, Brisbane QLD 4072 Australia

CORRESPONDING AUTHOR: Quoc Hung Dang (e-mail: quochung.dang@adelaide.edu.au).

ABSTRACT Tuning range extension strategies for varactor-based frequency-reconfigurable planar patch antennas are presented. The three tuning range optimization methods described in the paper include co-optimization of antenna dimensions and varactor properties, exploitation of multiple radiation modes, and reduction of parasitic capacitance. The first two strategies are emphasized by briefly reviewing two previously reported wide tuning range frequency-agile planar antennas. Importantly, the influence of parasitic capacitance on reducing the tuning range of the varactor-based frequency-reconfigurable antennas is then demonstrated by examining two antennas. The three tuning range extension methods are then combined to further expand the frequency tuning range of a reported frequency-reconfigurable antenna. The antenna has been re-designed, fabricated and experimentally characterized to demonstrate enhanced performance, which validates the proposed techniques, and their simultaneous application to reconfigurable antenna designs.

INDEX TERMS Antenna efficiency, frequency-reconfigurable antenna, tuning range extension.

I. INTRODUCTION

THE past 15 years have witnessed substantial progress in reconfigurable antennas. These developments have aimed at increasing versatility in operation or at extending capability to provide multi-functionalities in a single device [1]. Numerous advanced techniques have been proposed for reconfigurable antennas, with the aim of achieving reconfigurability in pattern [2]–[6], polarization [7]–[11], operation frequency [12]–[16] and/or the combination between several of these agility features [17]–[21]. Among them, frequency-reconfigurable antennas have arguably received the most significant attention from the very early development stages. This is due to the typical requirements of devices operating in different wireless standards [22]. This paper examines a fundamental aspect in frequency-reconfigurable antennas, which is the maximization of tuning range, TR, defined as

$$TR = 2\frac{f_{\max} - f_{\min}}{f_{\max} + f_{\min}} \times 100\%, \quad (1)$$

where $f_{\min}$ and $f_{\max}$ are the minimum and maximum operation frequencies, respectively.

In the literature, the tuning range is commonly optimized for a specific antenna structure. Among reconfigurable antennas proposed in the past, slot antennas were typically found to provide the widest reported frequency tuning, with fractional ranges reaching above 50% [23]–[26]. The main disadvantage of this antenna type is its difficulty of integration onto platforms. By contrast, planar antennas with a full ground plane and unidirectional patterns usually achieve a lower tuning range of around 13−35% [27]–[30]. Several designs have been previously reported with extended tuning range for reconfigurable microstrip patch antennas on full ground planes. In [31], a general framework for maximizing the tuning range and efficiency of a microstrip patch antenna was proposed. After optimization, a wide frequency tuning range of 41.5% was achieved. This range was among the best demonstrated for patch antennas at the time. Then in [21] and [32], continuous transitions between two radiation modes were exploited to further extend the fractional frequency tuning range to 57.3% and 70%, respectively, while keeping full ground planes and unidirectional radiation characteristics.

This paper aims to provide a systematic view of the tuning range extension strategies and optimization techniques for planar varactor-based frequency-reconfigurable antennas. Three main strategies, with the third one is the main contribution of this paper, are identified as

1) Choosing the dimensions and number of varactors that maximize the tuning range for a given capacitance range.
2) Utilizing multiple radiation modes with compatible radiation characteristics.
3) Reducing the parasitic capacitances.

The above techniques will be firstly explained by using design examples from the literature (Section II and III). Then, an antenna that combines all of those techniques will be demonstrated in Section IV, as a design example to validate the findings. The paper is not intended to offer a literature review, it rather aims at providing the readers, especially designers of reconfigurable antennas, an in-depth and systematic insight into the key approaches to maximize the tuning range. It is noted that the featured techniques can be used simultaneously as shown in a new proposed design in Section IV, which is also one of the main contributions of this work.

Since the tuning range is limited by the varactor capacitance range, for a consistent investigation and fair comparison, all designs presented in this paper use the same varactor type, i.e., MA120H46 with $[C_{\min}, C_{\max}] = [0.15, 1.30]$ pF with internal resistance of $R \approx 2\ \Omega$ [33]. It is emphasized that, the described methods can be however applied to other varactor types, with the presented findings remaining valid.

II. PREVIOUSLY REPORTED TUNING RANGE EXTENSION STRATEGIES

A. Optimization of Antenna Dimensions and Varactor Properties

Let us first consider a classical design of a frequency-reconfigurable planar antenna as presented in [31] (see the inset in Fig. 1). The antenna is excited by a probe feed and consists of two rectangular patches, i.e., a main patch and a tuning patch with the same length l, connected by a varactor diode. A design procedure was detailed in [31] and is graphically demonstrated in Fig. 1, which shows the relation between achievable resonance frequency tuning range and hypothetical value of varactor junction capacitance (from 0.001 to 1000 pF) for two different values of patch length l. The value of l are then identified according to the targeted frequency range (the lower the value of l, the higher the resonance frequencies achieved, as shown in Fig. 1). The number of parallel varactors is also part of the design, and it allows to adjust the capacitance range for a given commercially available varactor type. It can be observed from Fig. 1 that, at the value of $l = 18$ mm, the widest tuning range can be achieved by using three varactors.

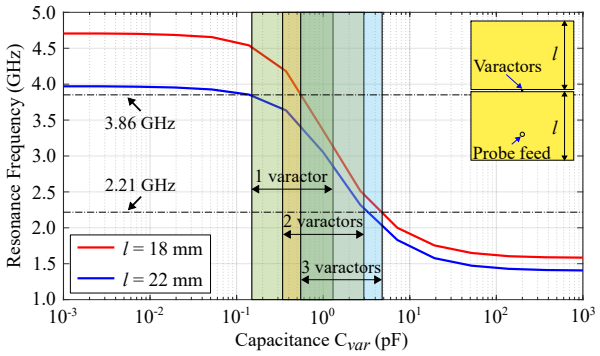

FIGURE 1. Simulated resonance frequencies of the antenna reported in [31] across different values of patch length and varactor capacitance. Inset: The considered classical design of a frequency-reconfigurable patch antenna.

The above method is applicable to almost all frequency-reconfigurable antenna and it has been applied successfully in various designs [19], [21], [30], [32], [33], leading to large tuning ranges. In general, the starting point is to plot the simulated resonance frequency graphs as a function of the varactor capacitance over a wide hypothetical range, in logarithmic scale, as illustrated in Fig. 1. This graphical representation provides an initial idea about a suitable varactor to be used and an estimation of the design dimensions. In-depth explanations of the method can be found in [31].

B. Exploitation of multiple radiation modes

In the previous example, a limitation on the tuning range is due to the appearance of parasitic resonances. This forces the design to limit its operation to a single mode, i.e., the fundamental mode of a patch. Interestingly, the design [32] overcomes this issue by utilizing a continous transition between two radiation modes, i.e., a quarter-wave planar inverted-F antenna (PIFA) mode and a half-wave patch mode. This can be observed in Fig. 2 where the simulated reflection coefficients and instantaneous electric field distribution of the antenna at two extreme frequencies within its tuning range are illustrated. Both radiation modes at 1.86 and 3.79 GHz are the lowest-order resonance mode of the structure (for a particular capacitance values C), thus parasitic higher-order resonances are avoided and a very large tuning range of 70% was obtained.

Compared to the design in Section II, a significant improvement in the tuning range (from 41.5% to 70%) is observed. Nevertheless, additional investigations reveal that such an improvement is not just due to the two-mode operation. If we optimize the antenna in [32] with the same substrate as in the antenna in [31], the optimized tuning range reaches only 55% with the lowest radiation efficiency at the lowest resonance frequency of approximately 23%. Therefore, another effect is at play here, which is related to the fact that the antenna in [32] utilizes an air-like foam substrate. The next section will reveal the reason behind this apparent discrepancy.

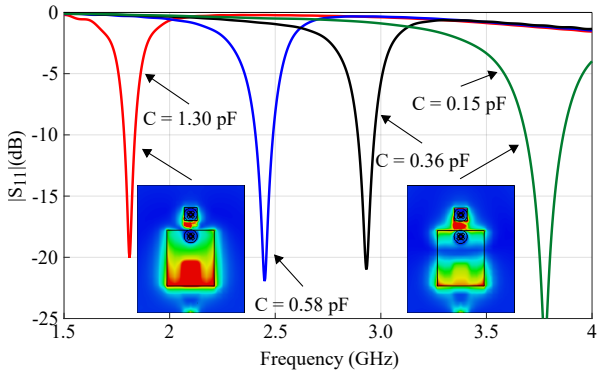

FIGURE 2. Simulated reflection coefficients of the antenna reported in [32]. Inset: instantaneous electric field distribution at the lowest and the highest resonance frequencies.

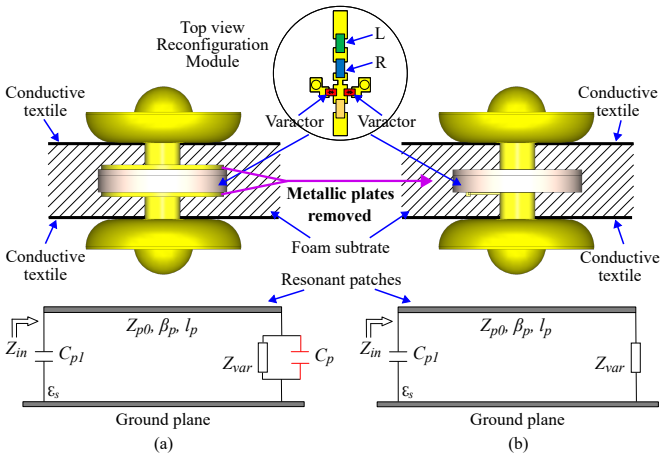

FIGURE 3. Antenna conceptual diagram with (a) a normal reconfiguration module and (b) an ideal module with removed male snap-on button bases.

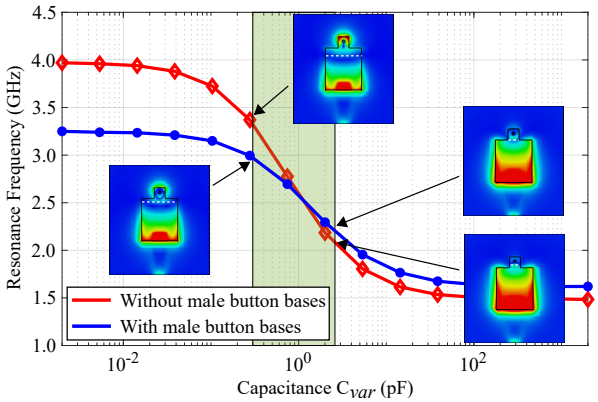

FIGURE 4. Simulated resonance frequency across different hypothetical values of varactor capacitance for the antenna in [30].

III. REDUCTION OF PARASITIC CAPACITANCE

It is found that parasitic capacitance plays a significant role in reducing the tuning range of varactor-based frequency-reconfigurable antennas. In this section, two frequency-reconfigurable antennas are examined to illustrate the effects of parasitic capacitance on the frequency tuning range.

A. Frequency-reconfigurable wearable patch antenna with vertical reconfiguration module

Let us first consider the frequency-reconfigurable textile antenna previously reported in [30]. This antenna configuration is similar to the antenna in [32], i.e., shown as the inset of Fig. 2, which includes a rectangular patch, a full ground plane, a proximity-coupled feed and a vertical reconfiguration module. In terms of operation mode, different from [32], this antenna only radiates in its quarter-wave mode within the tuning range. This antenna is chosen for investigation due to its strong parasitic capacitance effect.

Two configurations of the reconfigurable module are considered (see Fig. 3): (i) the original design in [30] and (ii) a modified design with the bases of the male snap-on buttons being removed. In the original design, the patch and the ground plane are connected through the impedance Z_{var} of the varactor, in parallel with C_p which is the parasitic capacitance of the module (see equivalent circuit in Fig. 3(a)). The parasitic capacitance C_p is mainly caused by the two male snap-on button bases placed on two sides of the module. In the modified design, C_p is drastically reduced and becomes negligible.

Due to the parasitic capacitance C_p, the range of the actual tuning capacitance becomes $[C_{\min}+C_p, C_{\max}+C_p]$. This effectively reduces the ratio between the maximum and minimum capacitance, since $(C_{\max}+C_p)/(C_{\min}+C_p) < C_{\max}/C_{\min}(C_p>0)$. Thus, a large value of C_p can severely affect the tuning range. This is confirmed by the electric field distributions, as well as the resonance frequency curves shown in Fig. 4. Without the parasitic capacitance, the loading effect of the varactor is more noticeable, especially at the higher resonance frequency. Consequently, by removing the parasitic capacitance caused by the male snap-on button bases, the frequency tuning range of the antenna is improved from 32.8% up to 47.2% (Fig. 4).

B. Frequency-reconfigurable patch antenna with co-planar reconfiguration module

As another example illustrating the severe effect of the parasitic capacitance, the antenna with 70% tuning range presented in [32] is re-considered. This time, a modification has been made, which substantially increases the parasitic capacitance: a conductive layer is added as ground plane to the reconfiguration module as displayed in Fig. 5(a) and (b).

The antenna equivalent circuit for the two cases are shown in Fig. 5(c) and (d), respectively. For convenience, these two antennas are called Ant. I (without the module's back copper layer) and Ant. II (with the module's back copper layer). The difference between these two cases arises from the parasitic capacitance C_{p3} appearing between the bottom copper layer and the top layer of the reconfiguration module (Fig. 5(d)). The resonance frequency obtained from full-wave simulations for different values of capacitance of a single (hypothetical) varactor from 0.001 to 1000 pF is displayed

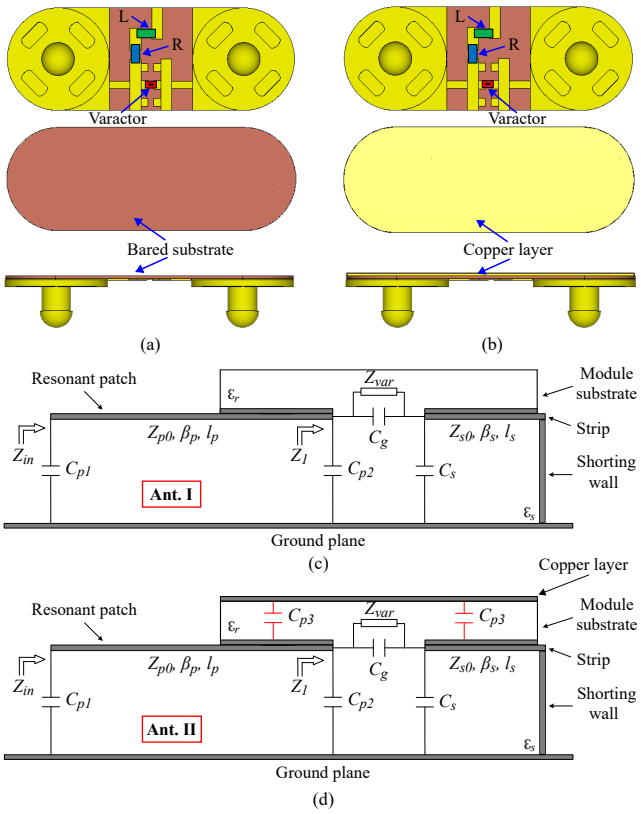

FIGURE 5. **Co-planar reconfiguration modules (a) without and (b) with added back copper layer. Equivalent circuit for antenna in [32] while using the reconfiguration module (c) without (Ant. I) and (d) with a back copper layer (Ant. II).**

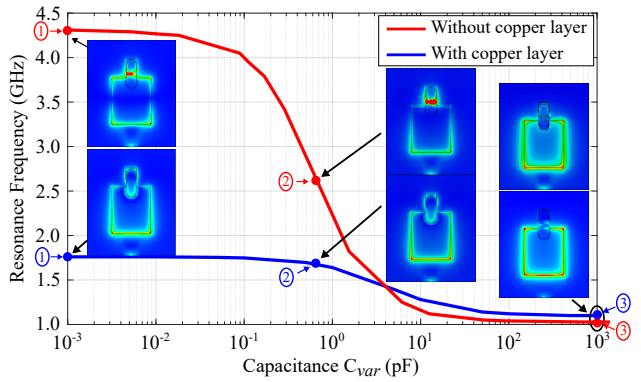

FIGURE 6. **Frequency-reconfigurable wearable textile antenna using co-planar reconfiguration module. Inset: Instantaneous electric field distribution of the antenna in the two cases at the lowest, the middle and the highest resonance frequency.**

in Fig. 6. The instantaneous electric field distribution at the lowest, middle and highest resonances of the two cases are also illustrated in the insets of Fig. 6. It can be observed that the tuning range of Ant. II is significantly reduced compared to the original design Ant. I.

The significant difference in the tuning range between Ant. I and Ant. II can be explained as follows. At the highest value of the varactor capacitance, the loading effect is the highest, and the two antennas are operating in their PIFA radiation mode ③ with the similar resonance frequency of approximately 1.0 GHz (see Fig. 6). When the varactor capacitance is decreased, the loading effect of the module in Ant. I is reduced accordingly while it is not decreased as significantly for Ant. II. This is because the tuning does not only depend on the varactor capacitance, but also on the fixed parasitic capacitance between the two copper layers of the module, i.e., $\approx 2C_{p3}+C_g$. That is, Ant. II is always radiating in its PIFA mode at all varactor capacitance values, as shown in the insets corresponding to the blue curve. In contrast, since the loading effect of the varactor in Ant. I decreases to a very low value, a nearly open-circuit condition appears. Consequently, the continuous transition between the PIFA and half-wave patch modes can be achieved, which extends the tuning range significantly.

C. Remarks

Both designs have illustrated the strong impact of parasitic capacitance in the tuning range of frequency-reconfigurable antennas. This effect has been often ignored in the literature, since it is inherently present in a selected structure. Nevertheless, being aware of this effect can guide design modifications to extend the tuning range in a particular structure. This will be illustrated in an example shown in Section IV.

This effect also explains why the antenna in [32] has much wider tuning range than the antenna in [31], namely 70.0% compared to 41.5%. The increased range is not just due to the two-mode operation but also to the fact that using lower-permittivity substrate will yield a smaller parasitic capacitance. It can be concluded that generally, using a lower-permittivity substrate will provide a larger tuning range for a same structure geometry. Thus, for a fair comparison, the substrate permittivity should be explicitly mentioned when comparing two frequency-reconfigurable antennas.

IV. DESIGN EXAMPLE

In this section, a design combining of all the above mentioned tuning optimization methods is demonstrated, aiming to further improve the tuning range of a reported frequency-reconfigurable antenna [31]. It is noted that the same rigid substrate with relative permittivity of 2.2 and the same number of varactor diodes will be used for a fair comparison. Furthermore, we also ensure that both antennas have the same lowest radiation efficiency, i.e., chosen here as 30% without restriction to generality. It is emphasized that such a task is very challenging as the design in [31] is among the best performance for planar antennas with unidirectional broadside patterns.

A. Antenna Structure

The antenna geometry is based on the PIFA structure as shown in Fig. 7, with all dimensions listed in the caption. The antenna consists of a main patch, a shorted tuning patch,

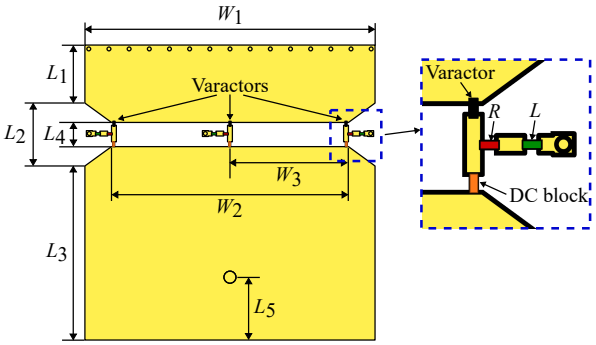

FIGURE 7. **Structure of the proposed reconfigurable microstrip antenna. Dimension (mm): L_1 = 6.0 mm, L_2 = 6.5 mm, L_3 = 18.0 mm, L_4 = 2.5 mm, L_5 = 6.5 mm, W_1 = 30.0 mm, W_2 = 24.5 mm, W_3 = 12.0 mm. Inset: zoomed-in bias circuit.**

shorting vias, a probe feed, a substrate and a full ground plane. The substrate material and dimensions are selected similar to the antenna reported in [31], which was Rogers Duroid 5880. The antenna is designed and optimized using CST Microwave Studio 2021.

B. Antenna Design Procedure

The design procedure is shown in Fig. 8, which consists of five steps. As described in Section II.B, we can first consider realizing one more compatible radiation mode beside the half-wave patch mode. Therefore, as first step, a shorting-via wall is added on the tuning patch as shown in Fig. 8(a). In the new design, the tuning patch length is then appropriately selected to excite the highest resonance frequency of approximately 4.0 GHz, which is similar to that of the original antenna [31]. By shorting the tuning patch, the quarter-wave radiation mode is excited through introduction of an electric wall symmetry, which also suppresses the even modes. The parametric optimization can follow the general method explained in Section II.A.

After adding the shorting wall with parameter optimization at Step 1, the tuning range extends from 2.3 to 4.0 GHz corresponding to 53.2% approximately. However, the antenna radiation efficiency at the lowest resonance frequency is limited to 23%. It is worth mentioning that, only the antenna radiation efficiency at the lowest frequency needs to be considered in the optimization process, since it corresponds to the minimum value. This minimum occurs at the highest varactor capacitance, which leads to maximum current flowing through the varactors.

As the next step, the distance of the varactor is re-optimized to achieve highest antenna radiation efficiency (Fig. 8(b)). As discussed in [31], by varying the distance in-between the varactors, the peak current through the varactors will change. This leads to a variation of the total varactor loss, which is the main contributor to the radiation efficiency reduction. The relation between the total losses in the lumped components and their distance (d_v) is illustrated in Fig. 9. It can be observed that, at the distance of 12 mm, the lowest total loss is obtained at approximately 0.235 W.

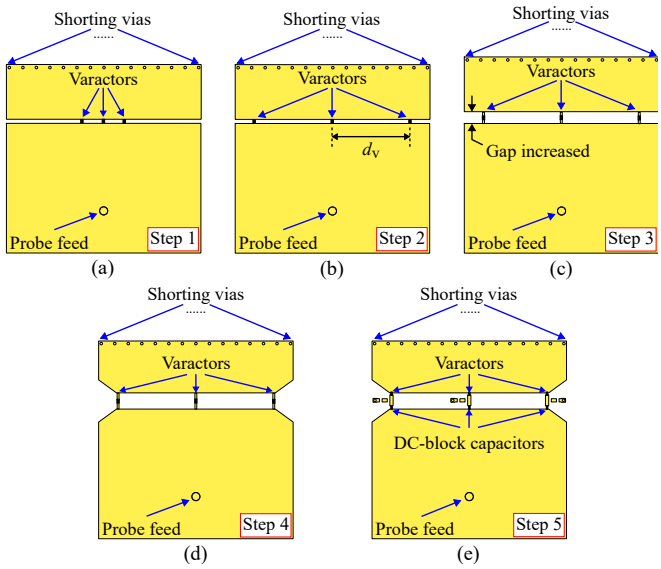

FIGURE 8. **Antenna design procedure for frequency tuning range extension. (a) Initial design with shorted parasitic patch, (b) optimization of the distance between the varactors, (c) reduction of parasitic capacitance between the patches, (d) further parasitic capacitance reduction through corner truncation, and (e) addition of the biasing circuit.**

Here, by changing the varactor distance from 2.4 mm to 12.0 mm, the total loss is decreased from 0.280 to 0.235 W. Correspondingly, the lowest radiation efficiency is increased from 23% to 40%. However, the lowest resonance frequency is increased from 2.30 to 2.69 GHz which reduces the tuning-range to 42%.

In the two previous steps, the multi-radiation mode and the varactor distance optimization have been implemented. In the third step, the reduction of the parasitic capacitance is considered. To this end, the gap in-between the main patch and the tuning patch is varied, as shown in Fig. 8(c), with the aim to reduce the parasitic capacitance between theses patches. However, a wider gap in-between the two patches reduces the minimum antenna radiation efficiency, as shown in Fig. 10. It can be observed from Fig. 10 that, the wider frequency tuning range corresponds to the lower radiation efficiency. The widest tuning range of approximately 80% is achievable at the cost of 7% radiation efficiency. Limiting the lowest antenna radiation efficiency to 30% as chosen design target, the distance between the two patches can be selected at 2.5 mm. This corresponds to the frequency tuning range of 51.2%. The two corners of each patch are truncated in Step 4 (see Fig. 8(d)) to further reduce the parasitic capacitance in-between the patches. By doing so, the frequency tuning range of the antenna is slightly increased to 52.7% while maintaining the radiation efficiency at 30%. The bias voltage circuit is then designed at the last step as shown in Fig. 8(e).

The instantaneous electric field distributions of the proposed antenna at four different resonance frequencies are shown in Fig. 11. The transition between the PIFA mode to the half-wave patch mode can be observed.

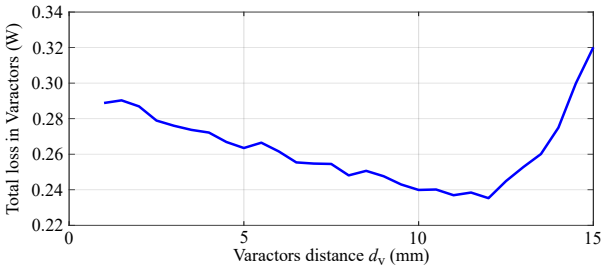

FIGURE 9. Simulated total losses in the three varactors for different distances between varactors for an input power of 0.5 W.

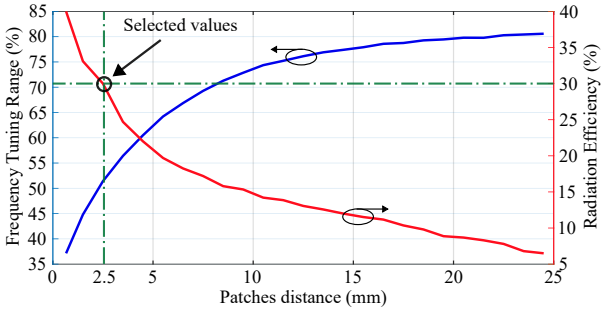

FIGURE 10. Simulated frequency tuning range and antenna radiation efficiency (at the lowest resonance frequency) for different distances between patches.

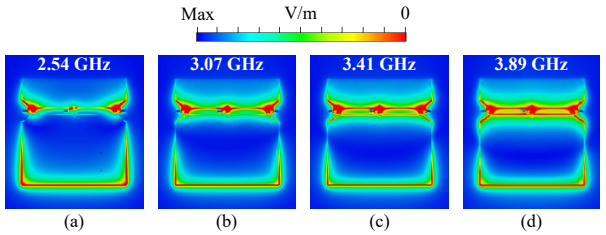

FIGURE 11. Instantaneous electric field distribution of the final design for the proposed frequency-reconfigurable antenna.

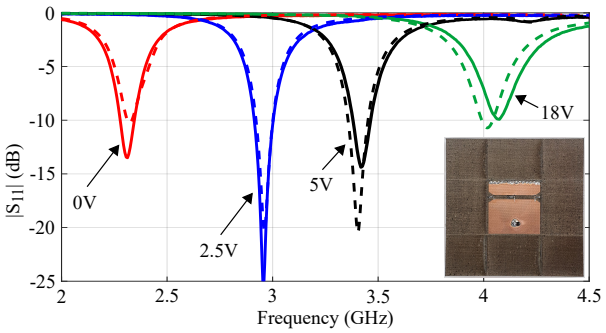

FIGURE 12. Simulated (dashed lines) and measured (solid lines) reflection coefficient of the proposed reconfigurable microstrip antenna. Inset: the fabricated antenna.

C. Experimental Results

Figure 12 shows the simulated and measured reflection coefficients of the proposed antenna, where a good agreement is obtained. The measured resonance frequency of the proposed antenna is varying from 2.31 to 4.08 GHz when the bias voltage is tuned from 0 to 18 V, which corresponds to a 55.8% fractional tuning range. Compared to the antenna presented in [31], the fractional tuning range is improved by approximately 14% for the same level of efficiency.

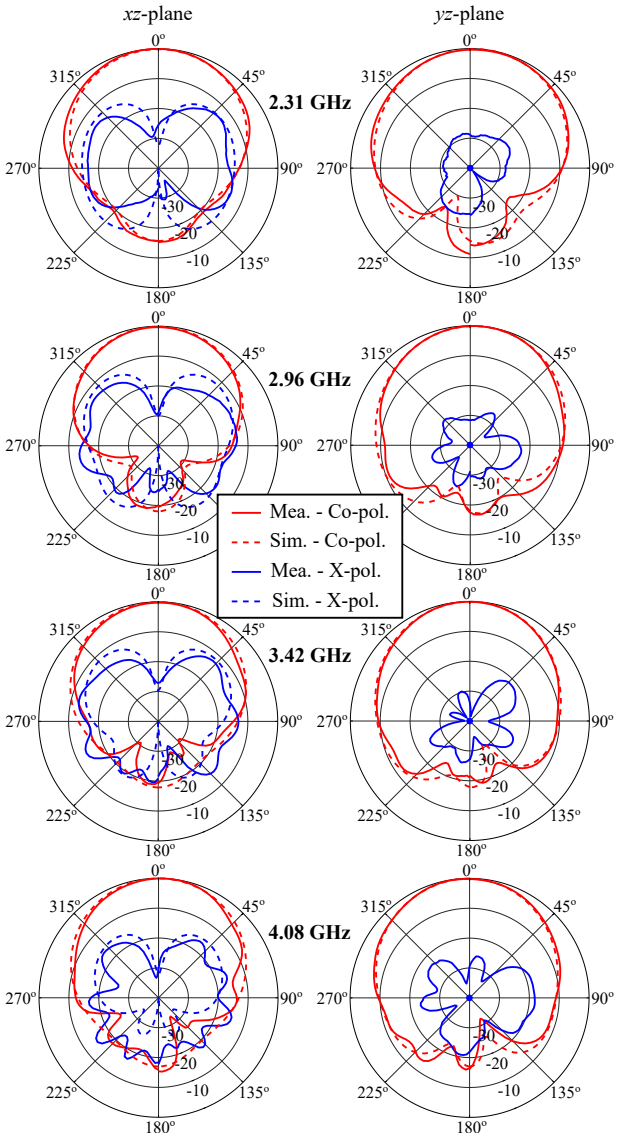

FIGURE 13. Simulated and measured normalized radiation patterns of the proposed reconfigurable microstrip antenna at 2.31, 2.96, 3.42 and 4.08 GHz.

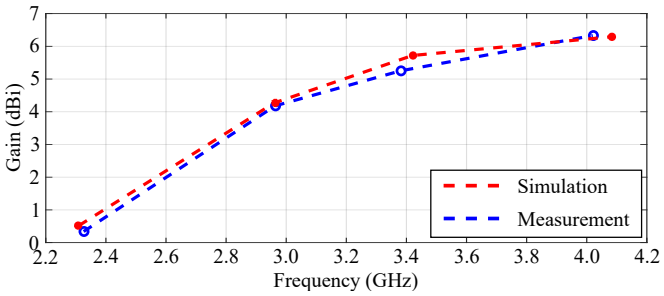

FIGURE 14. Simulated and measured gain of the proposed reconfigurable microstrip antenna at 2.31, 2.96, 3.42 and 4.08 GHz.

The normalized radiation patterns are displayed in Fig. 13. Across the frequency tuning range, stable broadside radiation patterns are obtained. The antenna realized gain is increasing from 0.52 to 6.29 dBi with increasing frequency within the tuning range, as illustrated in Fig. 14. The measured antenna radiation efficiency is estimated from the simulated one to range from 31.3% to 81.2% across the tuning range.

V. CONCLUSION

A procedure to extend the tuning range of a planar varactor-based frequency-reconfigurable antenna with consideration of radiation efficiency has been presented. The tuning-range extension strategies consist of two previously reported methods: (i) optimization of antenna dimensions and varactor properties, (ii) exploitation of multiple radiation modes, and one new method: (iii) minimization of parasitic capacitance at the varactor locations. The study particularly reveals one important feature that is often overlooked in frequency-reconfigurable antennas, namely that the parasitic capacitance can strongly affect the tuning range and thus the substrate permittivity can play a considerable role as well. The proposed approaches have been experimentally validated on a particular design, and show a generic pathway to optimize the tuning range of varactor-based planar antennas while considering the radiation efficiency. In comparison with a previously reported high-performing antenna [31], the re-optimized design exhibits approximately 14% wider tuning range while maintaining the same lowest radiation efficiency.

REFERENCES

[1] J. Costantine, Y. Tawk, S. E. Barbin, and C. G. Christodoulou, "Reconfigurable antennas: Design and applications," *Proc. IEEE,* vol. 103, no. 3, pp. 424–437, Mar. 2015.

[2] W. Lin, H. Wong, and R. W. Ziolkowski, "Wideband patternreconfigurable antenna with switchable broadside and conical beams," *IEEE Antennas Wirel. Propag. Lett.,* vol. 16, pp. 2638–2641, 2017.

[3] Z. Ding, R. Jin, J. Geng, W. Zhu, and X. Liang, "Varactor loaded pattern reconfigurable patch antenna with shorting pins," *IEEE Trans. Antennas Propag.,* vol. 67, no. 10, pp. 6267–6277, Jun. 2019.

[4] J. Hao, J. Ren, X. Du, J. H. Mikkelsen, M. Shen, and Y. Z. Yin, "Pattern-reconfigurable yagi-uda antenna based on liquid metal," *IEEE Antennas Wirel. Propag. Lett.,* vol. 20, no. 4, pp. 587–591, Apr. 2021.

[5] B. Mohamadzade, R. B. Simorangkir, R. M. Hashmi, R. Gharaei, A. Lalbakhsh, S. Shrestha, M. Zhadobov, and R. Sauleau, "A conformal, dynamic pattern-reconfigurable antenna using conductive textilepolymer composite," *IEEE Trans. Antennas Propag.,* vol. 69, no. 10, pp. 6175–6184, Oct. 2021.

[6] Y. Yuan, S. J. Chen, and C. Fumeaux, "Varactor-based phase shifters operating in differential pairs for beam-steerable antennas," *IEEE Trans. Antennas Propag.,* vol. 70, no. 9, pp. 7670 – 7682, 2022.

[7] C. Y. D. Sim, Y. J. Liao, and H. L. Lin, "Polarization reconfigurable eccentric annular ring slot antenna design," *IEEE Trans. Antennas Propag.,* vol. 63, no. 9, pp. 4152–4155, Sep. 2015.

[8] Q. Chen, J. Y. Li, G. Yang, B. Cao, and Z. Zhang, "A polarization reconfigurable high-gain microstrip antenna," *IEEE Trans. Antennas Propag.,* vol. 67, no. 5, pp. 3461–3466, May. 2019.

[9] K. Y. Kapusuz, S. Lemey, and H. Rogier, "Multipolarization-reconfigurable air-filled substrate integrated waveguide cavity-backed slot antenna," *IEEE Antennas Wirel. Propag. Lett.,* vol. 20, no. 4, pp. 622–626, Apr. 2021.

[10] D. Chen, Y. Liu, S. L. Chen, P. Y. Qin, and Y. J. Guo, "A wideband high-gain multilinear polarization reconfigurable antenna," *IEEE Trans. Antennas Propag.,* vol. 69, no. 7, pp. 4136–4141, Jul. 2021.

[11] M. C. Tang, Q. Lin, M. Li, and R. W. Ziolkowski, "Polarization-reconfigurable yagi-configured electrically small antenna," *IEEE Trans. Antennas Propag.,* vol. 69, no. 3, pp. 1757–1762, Mar. 2021.

[12] N. Nguyen-Trong, A. Piotrowski, and C. Fumeaux, "A frequency-reconfigurable dual-band low-profile monopolar antenna," *IEEE Trans. Antennas Propag.,* vol. 65, no. 7, pp. 3336–3343, Jul. 2017.

[13] M. Su, X. Geng, Y. Zhang, and A. Wang, "Frequency-reconfigurable liquid metal magnetoelectric dipole antenna," *IEEE Antennas Wirel. Propag. Lett.,* vol. 20, no. 12, pp. 2481–2485, Dec. 2021.

[14] S. C. Tang, X. Y. Wang, and J. X. Chen, "Low-profile frequency-reconfigurable dielectric patch antenna and array based on new varactor-loading scheme," *IEEE Trans. Antennas Propag.,* vol. 69, no. 9, pp. 5469–5478, Sep. 2021.

[15] T. K. Nguyen, C. D. Bui, A. Narbudowicz, and N. Nguyen-Trong, "Frequency-reconfigurable antenna with wide- and narrow-band modes for sub-6 GHz cognitive radio," *IEEE Antennas Wirel. Propag. Lett.,* vol. 22, no. 1, pp. 64–68, Jan. 2023.

[16] S. C. Tang, X. Y. Wang, S. Y. Zheng, Y. M. Pan, and J. X. Chen, "Frequency-reconfigurable dielectric patch antenna with bandwidth enhancement," *IEEE Trans. Antennas Propag.,* vol. 70, no. 4, pp. 2510–2519, Apr. 2022.

[17] N. Nguyen-Trong, L. Hall, and C. Fumeaux, "A frequency- and polarization-reconfigurable stub-Loaded microstrip patch antenna," *IEEE Trans. Antennas Propag.,* vol. 63, no. 11, pp. 5235–5240, Nov. 2015.

[18] Y. Liu, Q. Wang, Y. Jia, and P. Zhu, "A frequency- and polarization-reconfigurable slot antenna using liquid metal," *IEEE Trans. Antennas Propag.,* vol. 68, no. 11, pp. 7630–7635, Nov. 2020.

[19] S. N. M. Zainarry, S. J. Chen, and C. Fumeaux, "A frequency-reconfigurable single-feed zero-scanning antenna," *IEEE Trans. Antennas Propag.,* vol. 71, no. 2, pp. 1359 – 1368, Feb. 2022.

[20] L. Li, X. Yan, H. C. Zhang, and Q. Wang, "Polarization- and frequency-reconfigurable patch antenna using gravity-controlled liquid metal," *IEEE Trans. Circuits Syst. II Express Briefs,* vol. 69, no. 3, pp. 1029–1033, Mar. 2022.

[21] Q. H. Dang, S. J. Chen, N. Nguyen-Trong, and C. Fumeaux, "Multifunctional reconfigurable wearable textile antennas using coplanar reconfiguration modules," *IEEE Trans. Antennas Propag.,* vol. 71, no. 5, pp. 3806-3815, May 2023.

[22] P. Nepa and H. Rogier, "Wearable antennas for off-body radio links at VHF and UHF bands: challenges, the state of the art, and future trends below 1 GHz," *IEEE Antennas Propag. Mag.,* pp. 30–52, Oct. 2015.

[23] N. Behdad and K. Sarabandi, "Dual-band reconfigurable antenna with a very wide tunability range," *IEEE Trans. Antennas Propag.,* vol. 54, no. 2, pp. 409–416, Feb. 2006.

[24] H. Li, J. Xiong, Y. Yu, and S. He, "A simple compact reconfigurable slot antenna with a very wide tuning range," *IEEE Trans. Antennas Propag.,* vol. 58, no. 11, pp. 3725–3728, Nov. 2010.

[25] H. A. Majid, M. K. Abdul Rahim, M. R. Hamid, N. A. Murad, and M. F. Ismail, "Frequency-reconfigurable microstrip patch-slot antenna," *IEEE Antennas Wirel. Propag. Lett.,* vol. 12, pp. 218–220, 2013.

[26] R. Hussain, A. Ghalib, and M. S. Sharawi, "Annular slot-based miniaturized frequency-agile MIMO antenna system," *IEEE Antennas Wirel. Propag. Lett.,* vol. 16, pp. 2489–2492, Jul. 2017.

[27] S. L. S. Yang, A. A. Kishk, and K. F. Lee, "Frequency reconfigurable U-slot microstrip patch antenna," *IEEE Antennas Wirel. Propag. Lett.,* vol. 7, pp. 127–129, 2008.

[28] Lei Ge and Kwai-Man Luk, "Frequency-reconfigurable low-profile circular monopolar patch antenna," *IEEE Trans. Antennas Propag.,* vol. 62, no. 7, pp. 3443–3449, Jul. 2014.

[29] L. Ge, M. Li, J. Wang, and H. Gu, "Unidirectional dual-band stacked patch antenna with independent frequency reconfiguration," *IEEE Antennas Wirel. Propag. Lett.,* vol. 16, pp. 113–116, 2017.

[30] S. J. Chen, D. C. Ranasinghe, and C. Fumeaux, "A robust snap-on button solution for reconfigurable wearable textile antennas," *IEEE Trans. Antennas Propag.,* vol. 66, no. 9, pp. 4541–4551, Sep. 2018.

[31] N. Nguyen-Trong and C. Fumeaux, "Tuning range and efficiency optimization of a frequency-reconfigurable patch antenna," *IEEE Antennas Wirel. Propag. Lett.,* vol. 17, no. 1, pp. 150–154, Jan. 2018.

[32] Q. H. Dang, S. J. Chen, D. C. Ranasinghe, and C. Fumeaux, "A frequency-reconfigurable wearable textile antenna with one-octave

tuning range," *IEEE Trans. Antennas Propag.,* vol. 69, no. 12, pp. 8080–8089, Dec. 2021.

[33] N. Nguyen-Trong, T. Kaufmann, L. Hall, and C. Fumeaux, "Analysis and design of a reconfigurable antenna based on half-mode substrate-integrated cavity," *IEEE Trans. Antennas Propag.,* vol. 63, no. 8, pp. 3345–3353, Aug. 2015.

Quoc Hung Dang(S'18-M'23) received the M.E. and Ph.D. degrees in electrical and electronic engineering from the University of Adelaide, Australia, in 2018 and 2022, respectively.

Since August 2022, he has been working as a postdoctoral researcher in the School of Electrical and Electronic Engineering, The University of Adelaide. His current research interests include wearable, reconfigurable textile antennas, transparent antennas RFID-based wearable applications, material characterization.

Dr. Dang received a number of scholarship, travel grand including Adelaide Graduate Research Scholarship, the 2022 IEEE AP-S C. J. Reddy Travel Grant for Graduate Students and some Supplementary Scholarships. He was also awarded The Best Student Paper at the 2022 International Symposium on Antennas and Propagation (ISAP2022).

Dr. Dang has served as a reviewer for a number of recognized journals including the IEEE Transactions on Antennas and Propagation, the IEEE Antennas and Wireless Propagation Letters, the IEEE Sensors Journal and the Microwave and Optical Technology Letters.

Nghia Nguyen-Trong(M'17–SM'23) received the Ph.D. degree with Doctoral Research Medal in electrical engineering from The University of Adelaide, Adelaide, SA, Australia, in 2017.

From 2017 to 2020, he was a Postdoctoral Researcher at The University of Queensland, Australia. Since 2021, he has been a Lecturer with The University of Adelaide. His main research interests include microwave circuits, advanced materials, absorbers, and various types of antennas.

Dr. Nguyen-Trong was one of the recipients of the Best Student Paper Award at the 2014 IWAT, the 2015 IEEE MTT-S NEMO, and the 2017 ASA Conferences, and the Best Paper Award at the 2018 and 2020 Australian Microwave Symposium (AMS) Conferences. He has been continuously selected as a Top Reviewer for IEEE TRANSACTIONS ON ANTENNAS AND PROPAGATION, in 2018, 2019, 2020, and 2021, and IEEE ANTENNA WIRELESS AND PROPAGATION LETTERS, in 2018 and 2021. He serves as a Technical Co-Chair for the 2020, 2023 AMS and 2022 IEEE International Symposium on Antennas and Propagation (IEEE ISAP). He is listed among Australia's Top 40 Early Career Researchers by The Australian, November 2021.

Christophe Fumeaux(M'03–SM'09–F'19) received the Diploma and Ph.D. degrees in physics from the ETH Zurich, Switzerland, in 1992 and 1997, respectively.

From 1998 to 2000, he was a Postdoctoral Researcher with the School of Optics, University of Central Florida, Orlando. In 2000, he joined the Swiss Federal Office of Metrology, Bern, Switzerland, as a Scientific Staff Member. From 2001 to 2008, he was a Research Associate and Lecturer with the Laboratory for Electromagnetic Fields and Microwave Electronics at ETH Zurich. From 2008 to 2023, he has been a Professor with The University of Adelaide, Australia. In 2023, he joined the School of Electrical Engineering and Computer Science at The University of Queensland, as Chair Professor in Optical and Microwave Engineering. His main research interests concern applied electromagnetics, antenna engineering, and the application of RF design principles across the electromagnetic spectrum.

Prof. Fumeaux was the recipient of the ETH Medal for his doctoral dissertation. From 2011 to 2015, he was a Future Fellow of the Australian Research Council. He was the recipient of the 2018 Edward E. Altshuler Prize, the 2014 IEEE Sensors Journal and the 2004 ACES Journal best paper awards. He also received best conference paper awards at the 2012 Asia-Pacific International Symposium on Electromagnetic Compatibility (APEMC 2012) and the 17th Colloque International sur la Compatibilité Electromagnétique (CEM 2014). More than ten of his students have received student awards with joint papers at IEEE conferences. He was the recipient of the University of Adelaide Stephen Cole the Elder Award for Excellence in Higher Degree by Research Supervisory Practice in 2018. He served as an Associate Editor for the IEEE Transactions on Microwave Theory and Techniques from 2010 to 2013. From 2013 to 2016 he served as a Senior Associate Editor and later as the Associate Editor-in-Chief for the IEEE Transactions on Antennas and Propagation. From 2017 to early 2023, he served as the Editor-in-Chief for the IEEE Antennas and Wireless Propagation Letters.

Shengjian Jammy Chenreceived the M.E. and Ph.D. degrees in electrical and electronic engineering from The University of Adelaide, Australia, in 2013 and 2017 respectively.

From 2017 to 2021, he was a postdoctoral researcher and a lecturer in the School of Electrical and Electronic Engineering at The University of Adelaide. He joined the College of Science and Engineering at Flinders University, Australia, as a lecturer in 2022. His current research interests include antenna design and engineering, wearable technology, microwave absorbers, and electromagnetic structures using advanced materials.

Dr. Chen received scholarships including the Australian Postgraduate Award 2013 and the Simon Rockliff Scholarship 2015. He was also the recipient of several awards including the Young Scientist Best Paper Award at the International Conference on Electromagnetics in Advanced Applications (ICEAA) 2015, the Young Scientist Best Paper Award and Travel Bursary Award at ICEAA 2016, an Honorable Mention at IEEE AP-S Symposium on Antennas and Propagation (APS/URSI) 2017, a CST University Publication Award 2017, and the Best Paper Award at IEEE Asia-Pacific Microwave Conference 2021.

Dr. Chen was a Top Reviewer for IEEE Transactions on Antennas and Propagation in 2021 and 2023. He is an Associated Editor of IEEE Antennas and Wireless Propagation Letters. He was the Chair of the IEEE South Australia Joint Chapter on Microwave Theory and Techniques (MTT) & Antennas and Propagation (AP) from 2019 to 2020, and serves again since 2023.